LARGE EDDY SIMULATION OF THE TURBULENT FLOW PAST A BACKWARD FACING STEP WITH HEAT TRANSFER AND PROPERTY VARIATIONS

Ravikanth V.R. Avancha *
Department of Mechanical Engineering
Iowa State University
Ames IA 50011, USA
ark@iastate.edu

Richard H. Pletcher †
Department of Mechanical Engineering,
Iowa State University
Ames IA 50011, USA
pletcher@iastate.edu

ABSTRACT

The effects of heat transfer and property variations on the turbulent flow past a backward facing step are investigated using large eddy simulation. Heat transfer is achieved through a constant heat flux boundary condition downstream of the step. Upstream of the step, the flow is fully developed. The Reynolds number based on the step height and upstream centerline velocity is 5540 and the expansion ratio is 1.5. Prior to carrying out the simulations with heat transfer, an isothermal flow simulation was conducted and results show good agreement with the particle tracking velocimetry experiments of Kasagi and Matsunaga. A robust collocated grid finite volume scheme using central differences and a nonlinear filter to suppress numerical oscillations has been developed. A fully coupled compressible formulation employing low Mach number preconditioning is adopted for the simulations conducted on the CRAY T-90. A dynamic subgrid scale procedure applied to the compressible version of the Smagorinsky model has been used to capture the effects of the small scales.

INTRODUCTION

The objective of the current research is to develop LES technology to tackle complex separating and reattaching turbulent flows with heat transfer and property variations, characteristic of practical application areas. Such flows cause large variations of local heat transfer coefficient as well as augment overall heat transfer. Separated flow regions occur quite commonly in application areas related to combustors, aircraft propulsion equipment, and electronics cooling. Available experimental data are small in number, as indicated by Vogel and Eaton (1984). Experiments are also constrained by practical limitations to impose moderate heat flux levels, not quite close to the levels that are usually found in practical applications. As a result, the influence of heat transfer in regions of separated and reattaching flow is not well understood. In numerical simulations, it is possible to include desired heat flux levels, and temperature gradients. Most of the numerical calculations to date for this flow regime with heat transfer have used two equation turbulence models like the $k-\epsilon$ and $k-\omega$ models with the Reynolds averaged Navier-Stokes (RANS) equations. A summary of benchmark calculations carried out by Abrous and Emery (1996) noted that only the results for u-velocity and dissipation agreed amongst all contributors, but substantial differences were noted for the v-velocity, skin friction, Nusselt number, and wall temperatures. For the Nusselt number profiles, none of the methods produced a shape similar to the experimental results of Mori et al. (1986). There did not appear to be any consistency in the computed points of maximum Nusselt number and the reattachment point (Abrous and Emery, 1996). Simulations in-

*Graduate Research Assistant
†Professor

volving heat transfer have not included the effects of property variations although large heat flux levels have been used. Thus, the simulations presented in this work offer a way to better understand the effects of heat transfer and property variations in separated flow regions at low speeds.

MATHEMATICAL FORMULATION

Large eddy simulation involves the computation of the motion of large scale structures, and modeling of the effect of the nonlinear interactions with the small-scales. A filtering procedure applied to the Navier-Stokes (NS) equations serves the purpose of precisely defining the scales that would be resolved and the scales that would be modeled. For finite volume schemes, the finite grid resolution is an implicit top hat filter. Favre filtering is used for the compressible formulations of the NS equations. For a quantity ϕ, the Favre filtered quantity $\tilde{\phi}$ is defined as $\frac{\overline{\rho\phi}}{\overline{\rho}}$.

Governing Equations

The Favre-filtered compressible NS equations, in their non-dimensional form are given as:

$$\frac{\partial \overline{\rho}}{\partial t} + \frac{\partial \overline{\rho}\tilde{u}_j}{\partial x_j} = 0 \tag{1}$$

$$\frac{\partial \overline{\rho}\tilde{u}_i}{\partial t} + \frac{\partial \overline{\rho}\tilde{u}_i\tilde{u}_j}{\partial x_j} = -\frac{\partial \overline{p}}{\partial x_i} + \frac{\partial \overline{\sigma}_{ij}}{\partial x_j} - \frac{\partial \tau_{ij}}{\partial x_j} \tag{2}$$

$$\frac{\partial}{\partial t}(\overline{\rho}\tilde{T}) + \frac{\partial}{\partial x_j}(\overline{\rho}\tilde{u}_j\tilde{T}) = -\frac{\partial \overline{q_j}}{\partial x_j} - \frac{\partial Q_j}{\partial x_j} \tag{3}$$

where the viscous stress tensor and heat conduction vector are given as,

$$\overline{\sigma}_{ij} = \overline{\frac{\mu}{Re}\left(\frac{\partial u_i}{\partial x_j} + \frac{\partial u_j}{\partial x_i} - \frac{2}{3}\frac{\partial u_k}{\partial x_k}\delta_{ij}\right)} \tag{4}$$

$$\overline{q}_j = -\overline{\frac{k}{Pr\,Re}\left(\frac{\partial T}{\partial x_j}\right)} \tag{5}$$

and the subgrid (SGS) scale stress tensor and heat conduction vector are given as,

$$\tau_{ij} = \overline{\rho}(\widetilde{u_i u_j} - \tilde{u}_i\tilde{u}_j) \tag{6}$$

$$Q_j = \overline{\rho}(\widetilde{u_j T} - \tilde{u}_j\tilde{T}) \tag{7}$$

The turbulent stress τ_{ij} and the turbulent heat flux Q_j have to be modeled in order to close the system of equations, and these terms represent the effect of the subgrid scale velocity and temperature components on the evolution of the large-scales. The Favre filtered equation of state is

$$\overline{p} = \overline{\rho}R\tilde{T} \tag{8}$$

Variations of viscosity and conductivity are given by the power-law form of Sutherland's formula

$$\frac{\mu^*}{\mu_{ref}} = \left(\frac{T^*}{T_{ref}}\right)^{0.71}; \quad \frac{k^*}{k_{ref}} = \left(\frac{T^*}{T_{ref}}\right)^{0.71} \tag{9}$$

where the superscript '*' and subscript '*ref*' refer to dimensional and reference quantities respectively. The Prandtl number and specific heat at constant pressure C_p, are treated as constants for the temperature range in consideration.

Subgrid Scale Modeling

Smagorinsky model. The compressible flow version of the Smagorinsky model is given as

$$\tau_{ij} = \frac{1}{3}\tau_{kk}\delta_{ij} - 2\mu_T(\tilde{S}_{ij} - \frac{1}{3}\tilde{S}_{kk}\delta_{ij}) \tag{10}$$

where μ_T is the eddy-viscosity, and

$$\tilde{S}_{ij} = \frac{1}{2}\left(\frac{\partial \tilde{u}_i}{\partial x_j} + \frac{\partial \tilde{u}_j}{\partial x_i}\right) \tag{11}$$

is the Favre-filtered strain rate tensor. τ_{kk} is the sub-grid scale turbulent kinetic energy which needs to be modeled for the case of compressible flows. The model proposed by Yoshizawa (1986) can be written as

$$\tau_{kk} = 2C_I\bar{\rho}\Delta^2|\tilde{S}|^2 \tag{12}$$

For closure, μ_T is parameterized by equating the sub-grid scale energy production and dissipation, and the SGS heat flux vector Q_j is modeled using a gradient-diffusion hypothesis, to obtain

$$\mu_T = C_s\bar{\rho}\Delta^2\sqrt{2\tilde{S}_{ij}\tilde{S}_{ij}} \tag{13}$$

$$Q_j = -\frac{\bar{\rho}C_s\Delta^2|\tilde{S}|}{Pr_T}\frac{\partial \tilde{T}}{\partial x_j} \tag{14}$$

where C_s is a model parameter to be specified and Pr_T is the turbulent Prandtl number defined as the ratio of eddy-viscosity ν_T to eddy-diffusivity α_T. Δ is the filter width which is typically assumed to be a function of

the grid resolution, and calculated as $\Delta_{av} = (\Delta x \Delta y \Delta z)^{1/3}$.

Dynamic model procedure. The extension of the dynamic model for compressible flows proposed by Moin et al. (1991) has been used. The dynamic model procedure, in this study, employs the Smagorinsky model as its base model. The model parameter C_s, and Pr_T are calculated "dynamically" using spectral information from two different levels already part of the resolved solution. The procedure requires the definition of a new "test" filtering operation where the test filter $\hat{\Delta}$ is greater than the grid filter width, Δ. On application of the test filter to the filtered NS equations, one obtains the sub-test scale stress terms. The stresses at the two different filter levels are related by the algebraic identity of Germano (1992).

NUMERICAL PROCEDURE

A coupled finite volume procedure, in primitive variables $[p, u, v, w, T]$ was used to solve the filtered NS equations. The method was fully implicit, second order accurate in time, with advective terms discretizable using second order/fourth order central differences and viscous terms with fourth order central differences. Time derivative preconditioning (Pletcher and Chen, 1993) was incorporated to alleviate the stiffness and convergence problems associated with flows that occur with traditional compressible formulations at low Mach numbers. An all-speed strategy has thus evolved that enables the application of the same methodology to incompressible flows and compressible flows at low Mach numbers where effects of property variations need to be accounted for. Sixth order compact filtering (Lele, 1992) was used to eliminate the pressure-velocity decoupling peculiar to collocated-grid methods. The system of algebraic equations was solved using Stone's strongly implicit procedure (SIP) (Weinstein, 1969). A code well optimized for performance on the CRAY T-90 was used to perform the large eddy simulations.

LARGE EDDY SIMULATIONS

Flow conditions and geometry

The geometry of the domain of interest is shown in Fig.1. Reference values of some key variables were: $U = 2.063$ m/s, $k = 25.74 \times 10^{-3}$ W/m K, $L = 0.041$ m, $\nu = 15.27 \times 10^{-6}$ m^2/s, $T = 293.0$ K, and $\rho = 1.194$ kg/m^3. The grid resolution used for the simulations was: (1) Upstream of step: $17 \times 31 \times 48$, (2) Downstream of step: $72 \times 46 \times 48$ in the streamwise, wall-normal and spanwise directions respectively. Non-uniform grids were employed in the wall-normal (y), and streamwise (x) directions as opposed to a uniform grid in the spanwise (z) direction.

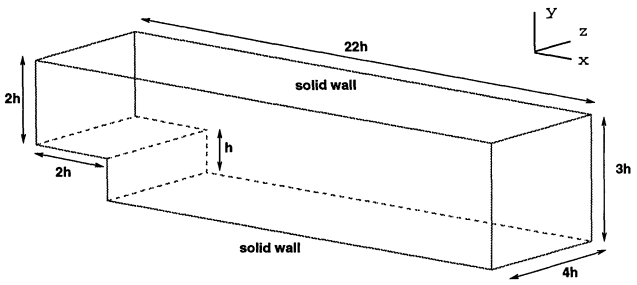

Figure 1: Backward-facing step geometry

Boundary conditions

No-slip boundary conditions were enforced at the top and bottom solid walls. Periodicity of flow was assumed in the spanwise direction. The Navier-Stokes characteristic boundary condition strategy (Poinsot and Lele, 1992) was employed at the inflow and outflow boundaries. Turbulent inflow conditions for each time step of the simulation were provided by planes of data stored from an independent LES of a channel flow with the same Reynolds number and time step. For the simulations with heat transfer, the bottom wall downstream of the step was the only one supplied with a constant heat flux. The remaining walls were insulated (adiabatic conditions).

Isothermal Flow Case

This simulation was designed to match the backward-facing step geometry from the particle tracking velocimetry (PTV) experiments of Kasagi and Matsunaga (1995). The Reynolds number based on the step height and upstream centerline velocity was 5540. The streamwise (Fig. 2), wall-normal (Fig. 3) and spanwise mean velocity distributions, and the respective root mean square fluctuations from the simulation showed excellent agreement with experimental results. Third order moments also showed good qualitative agreement with the experiment. The mean reattachment length from the simulation is predicted to be 6.0 x/h, as compared with the 6.51 x/h reported in the experiment. Details of the simulation and results have been presented by Avancha and

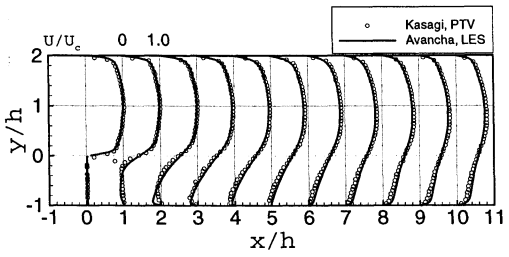

Figure 2: Mean streamwise velocity

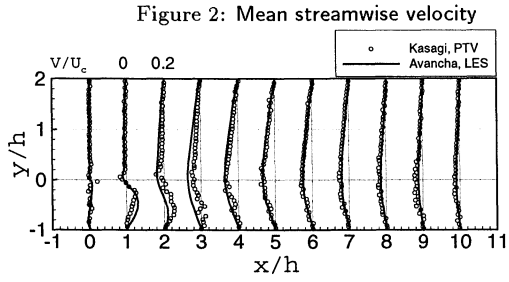

Figure 3: Mean wall-normal velocity

Pletcher (2000).

Constant Wall Heat Flux Cases

The geometry used for the isothermal simulations was retained with the hope that results from the LES would motivate new experimental work, in light of advances being made in measurement methods, to include the effects of heat transfer. Importantly, using the same geometry permits the use of the planes of channel flow data for inflow conditions, initial conditions for the heat transfer cases become easily available from the isothermal simulations, and result in significant savings in computer resources. Mean streamwise velocity and mean temperature profiles are shown in Figures 4 and 5.

Heat flux levels of $1\,\mathrm{kW/m^2}$, $2\,\mathrm{kW/m^2}$, $3\,\mathrm{kW/m^2}$ are supplied to the surface downstream of the step, yielding maximum T_{wall}/T_{bulk} ratios of about 1.7, 2.3, and 2.9 respectively. The bulk temperature profiles (Fig. 6) are in good agreement with analytical estimates. The wall temperatures (Fig. 7) show a dramatic increase downstream of the step, reaching their peak values in the neighborhood of the streamwise distance of 2 x/h. Upon inspection of the Nusselt number profiles (Fig. 8) we observe that this increase in temperature corresponds to a significant decrease in heat transfer close to the step - it is almost as if the air is in a "stagnant state". The wall temperature profiles then drop, possibly due to increased heat transfer in the reattaching region before showing a linear increase downstream of reattachment that corresponds to the growth of the thermal boundary layer. The

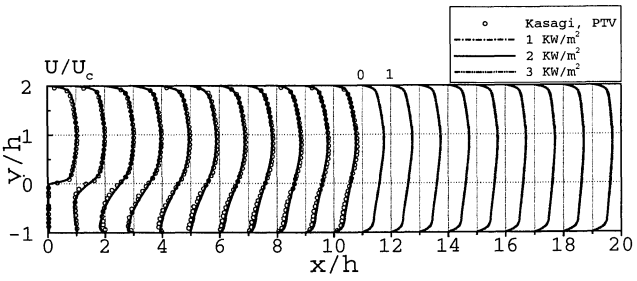

Figure 4: Mean streamwise velocity

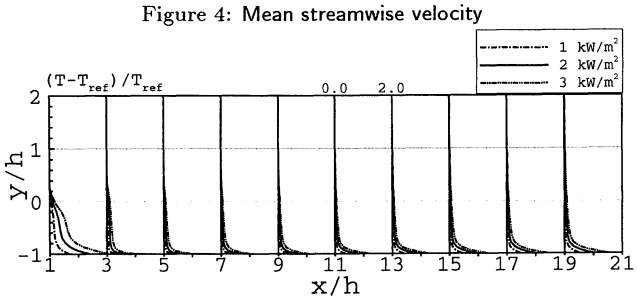

Figure 5: Mean temperature

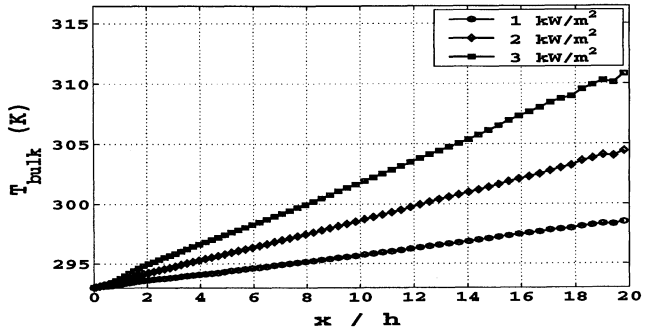

Figure 6: Bulk temperature

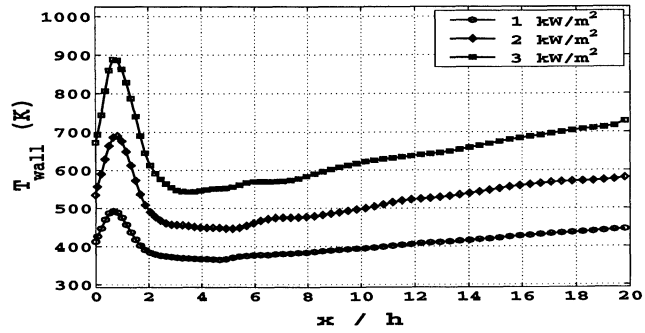

Figure 7: Wall temperature

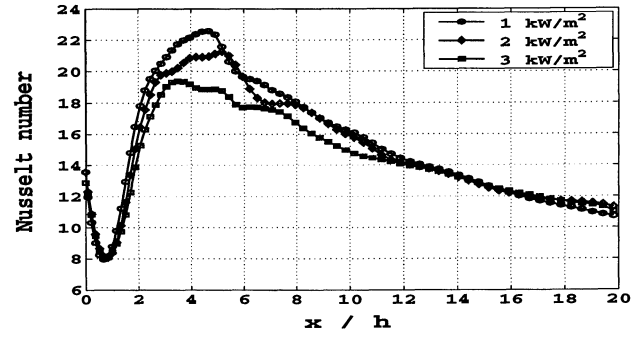

Figure 8: Nusselt number

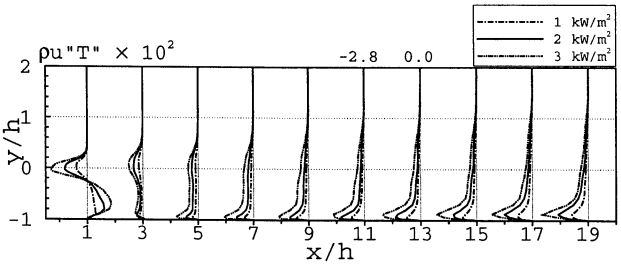

Figure 9: Streamwise turbulent heat flux

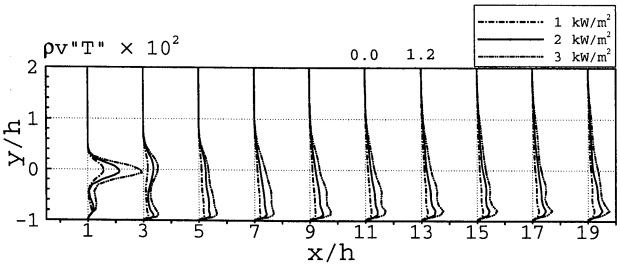

Figure 10: Vertical turbulent heat flux

Nusselt number attains a maximum slightly upstream of reattachment, which is in agreement with Vogel and Eaton (1984), as opposed to several other works which have placed it at the reattachment point. Upon comparison of the Nusselt number profiles for the three heat flux cases in the separation bubble region, with increasing heat flux, an increasing effect of conductive heat transfer as opposed to convective heat transfer in the recirculation region can be inferred. Downstream of reattachment, the Nusselt number profiles appear to resemble the flat plate boundary layer behavior. The growth of the thermal boundary layer is clearly discernible from examining the spread of the mean temperature gradients in Fig. 5. It is indicated in Vogel and Eaton (1984) that it might require well over 50 step heights for the downstream flow to reach a fully developed state.

Vogel and Eaton (1984) have indicated that the streamwise turbulent heat flux is negligible as compared to the wall-normal turbulent heat flux. However, we show that while the streamwise turbulent heat flux, as in Fig. 9, is indeed smaller in magnitude than the wall-normal turbulent heat flux, Fig. 10, nevertheless it is non-negligible. The heat flux levels in this work are an order of magnitude greater than in their work (130 W/m^2) and the Reynolds numbers are three to five times smaller. These are probable reasons for their observation of negligible streamwise turbulent heat flux in comparison with the vertical turbulent heat flux.

Root mean square density fluctuations of up to 20 % are observed in Fig. 11. At the

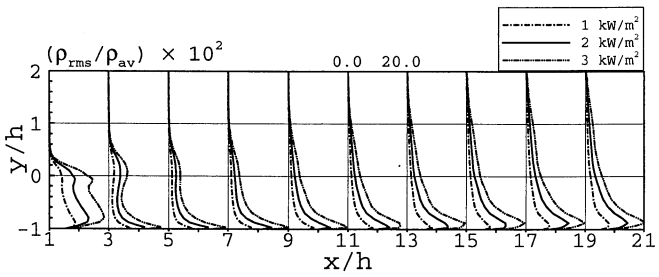

Figure 11: RMS density fluctuations

peak wall temperatures for the three heat flux cases, the viscosity and thermal conductivity are roughly about 20%, 40% and 60% greater than their reference values, thus demonstrating the need for property variations to be considered in calculations involving high heat fluxes. All the calculations included in the review by Abrous and Emery (1996) have used wall heat flux values of $5\,kW/m^2$ and relied on the assumption of constant properties.

While the Reynolds analogy does not hold in the mean sense in the recirculation region, it is possible that it might hold in an instantaneous sense. For this to be true, one would expect the mean Stanton number (Fig. 12) to be correlated with the time average of the absolute skin-friction (Fig. 13) - results from our simulation support this observation of Vogel and Eaton (1984). It is interesting to note that the mean Stanton number profiles (Fig. 12) show a striking similarity with the fluctuating skin-friction profiles (Fig. 14), than they do with the average absolute skin-friction (Fig. 13).

CONCLUDING REMARKS

Large eddy simulations to study the heat transfer and fluid dynamics of the turbulent reattaching flow past a backward-facing step have been successfully conducted. The choice of the formulation enabled the inclusion of property variations, and facilitated the study at low Mach numbers. An increase in heat flux supplied to the bottom wall downstream of the step results in the heat transfer rate starting to be dominated by conduction as opposed to convection. The peak heat transfer rate occurs slightly upstream of reattachment. Streamwise and wall-normal turbulent heat fluxes are of the same order of magnitude. Dramatic variation of the wall temperatures in the recirculation region is observed. The Stanton number profiles correlate strongly with the fluctuating skin-friction profiles. While the Reynolds analogy is not valid for a flow with separation and reattachment, the possibility of a "instanta-

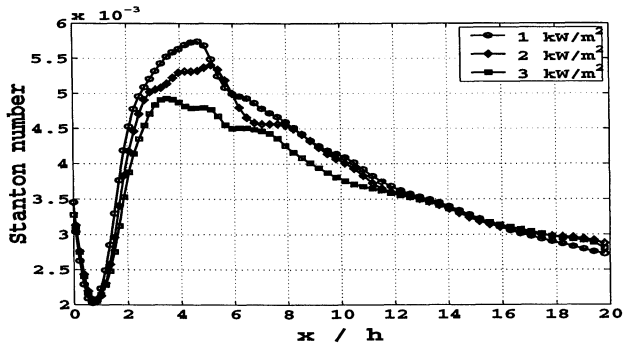

Figure 12: Mean Stanton number

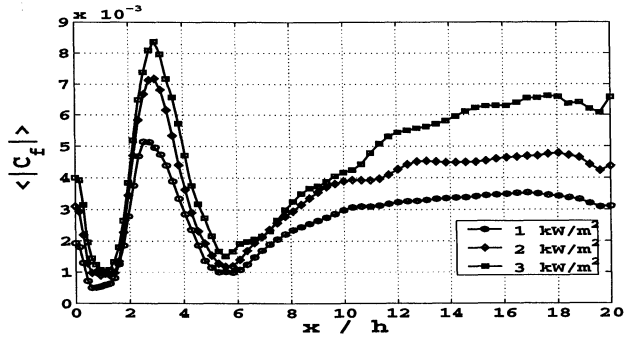

Figure 13: Average of absolute skin-friction

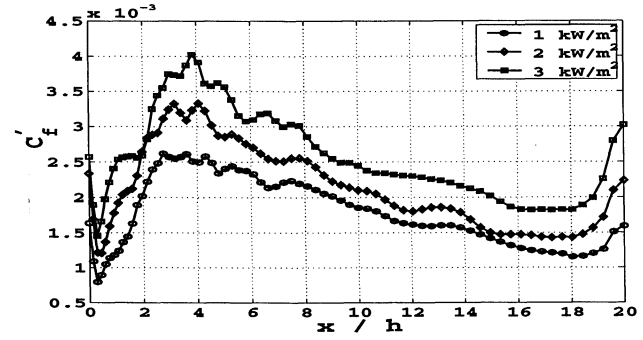

Figure 14: Fluctuating skin-friction

neous" Reynolds analogy corroborates with the observations of Vogel and Eaton (1984).

ACKNOWLEDGMENTS

The current research was partially supported by the Air Force Office of Scientific Research under Grant F49620-94-1-0168 and by the National Science Foundation under grants CTS-9414052 and CTS-9806989. The use of computer resources provided by the National Partnership for Advanced Computational Infrastructure at the San Diego Supercomputing Center is gratefully acknowledged.

REFERENCES

1. Abrous, A., and Emery, A. F., 1996, Benchmark computational results for turbulent backward-facing step flow with heat transfer, HTD-Vol. 331, National Heat Transfer Conference, Vol. 9, ASME.

2. Avancha, R., and Pletcher, R. H., 2000, Large eddy simulation of the turbulent flow past a backward facing step, AIAA 2000-0542, 38th Aerospace Sciences Meeting and Exhibit, 10-13 January 2000, Reno, NV.

3. Germano, M., 1992, Turbulence: the filtering approach, *Journal of Fluid Mechanics*, Vol. 238, pp. 325-336.

4. Lele, S., 1992, Compact finite difference schemes with spectral-like resolution, *J. Comp. Phys*, Vol. 103, pp. 16-42.

5. Moin, P., Squires, K., Cabot, W., and Lee, S., 1991, A dynamic subgrid scale model for large eddy simulations of compressible turbulent flows, *Phys. Fluids A*, Vol. 3, pp. 2746-2757.

6. Mori, Y., Uchida, Y. and Sakai, K., 1986, A study of the time and spatial structure of heat transfer performances near the reattaching point of separated flows, *Procs. 8th Int. Heat Transfer Conference*, pp. 1083-1088.

7. Pletcher, R. H. and Chen, K.-H., 1993, On solving the compressible Navier-Stokes equations for unsteady flows at very low Mach numbers, AIAA Paper 93-3368.

8. Poinsot, T. J., and Lele, S. K., 1992, Boundary conditions for direct simulations of compressible viscous flows, *J. Comp. Phys*, Vol. 101, pp. 104-129.

9. Kasagi, N., and Matsunaga, A., 1995, Three-dimensional particle-tracking velocimetry measurement of turbulence statistics and energy budget in a backward facing step flow, *Int. J. Heat and Fluid Flow*, Vol. 16, pp. 477-485.

12. Vogel, J. C., and Eaton, J. K., 1984, Heat transfer and fluid mechanics measurements in the turbulent reattaching flow behind a backward facing step, Report MD-44, Thermosciences Division, Department of Mechanical Engineering, Stanford University.

13. Wang, W.-P., 1995, Coupled compressible and incompressible finite volume formulations of the large eddy simulation of turbulent flows with and without heat transfer, Ph.D. Thesis, Iowa State University.

14. Weinstein, H. G., Stone, H. L., and Kwan, T. V., 1969, Iterative procedure for solution of systems of parabolic and elliptic equations in three dimensions. *I & E C Fundamentals*, Vol. 8, pp. 281-287.

15. Yoshizawa, A., 1986, Statistical theory for compressible turbulent shear flows, with the application to subgrid modeling. *Physics of Fluids A*, Vol. 5, pp. 3186-3196.